

## Plasmon satellite in the valence-band photoemission spectra of metals

Shyamalendu M. Bose

*Department of Physics and Atmospheric Science, Drexel University,  
Philadelphia, Pennsylvania 19104*

Steven Prutzer

*Department of Physics and Atmospheric Science, Drexel University,  
Philadelphia, Pennsylvania 19104  
and General Electric Company, 3198 Chestnut Street,  
Philadelphia, Pennsylvania 19101*

Pierre Longe

*Institut de Physique, B-5, Université de Liège, Sart-Tilman, B-4000 Liège, Belgium*  
(Received 16 October 1981)

The line shape and intensity of the first bulk plasmon satellite in the valence-band photoemission spectrum of a simple metal have been calculated. It is found that, owing to the mobility of the final-state hole created in the valence band, the magnitudes of the intrinsic and interference terms are altered from that found in the absence of such mobility, while the extrinsic contribution remains unaffected. The overall effect of the recoil is to reduce the total intensity of the plasmon band. In the case of excitation of a dispersionless plasmon, the satellite band basically reflects the parabolic main band in its line shape and width. For the plasmon excitation with dispersion and attenuation, the satellite band is weaker in strength, broader in width, and goes to zero smoothly at both upper- and lower-energy edges.

### I. INTRODUCTION

Recently, there have been extensive experimental<sup>1-5</sup> and theoretical<sup>6-11</sup> investigations of the core-level photoemission spectra of simple metals. The asymmetry of the main line has been explained on the basis of the Nozières—de Dominicis model. The intensities of the plasmon satellites and the background have been measured and calculated. These intensities are found to depend strongly on the incident photon energy. Most features are explained on the basis of three basic processes—*intrinsic, extrinsic, and interference*—that take place during the photoemission from the core state. For example, at low incident photon energies, the negative quantum interference term is large, but its magnitude decreases with increasing incident photon energy. Thus one expects to observe a lower intensity plasmon band and background at lower photon energies. These conclusions have been verified by several recent experimental observations.

Even though the core-level photoemission spectra of metals have been studied extensively, no

such systematic studies of the valence-band photoemission spectra of metals have been carried out. The basic processes that will govern the photoemission in this case are essentially the same as those of the core-level photoemission. However, one expects to observe a difference for at least two fundamental reasons. First, since an electron can be photoemitted from any level in the conduction band one expects to observe a wider photoemission band in this case. Of greater importance, since the final-state hole is created in the conduction band, it is able to recoil. This mobility of the final-state hole can modify the strength and shape of the photoemission spectra of simple metals. In a recent publication,<sup>12</sup> Hedin has used the hole propagator and the related spectral function to estimate the intrinsic contribution to the plasmon satellite. His calculation indicates that this contribution is weaker in the conduction state than in the core-state photoemission. Most recently, Longe and Bose<sup>13</sup> have calculated the effect of hole recoil on the integrated strength of the plasmon satellite and have found that recoil reduces the integrated strength by a significant amount. Previously,

Doniach<sup>14</sup> and McMullen *et al.*<sup>15</sup> proposed schemes for studying the effects of hole recoil. Doniach's study involved narrow  $d$  bands and the work of McMullen *et al.* was related to the electron-loss spectroscopy, not photoelectron spectra. Experimentally, some attempts have been made to measure the valence-band photoemission spectra of metals by several investigators.<sup>16,17</sup>

In this paper, we undertake a detailed study of the intensity and line shape of the plasmon satellite for photoemission from the conduction band of a simple metal. We are primarily interested in investigating how the three processes—*intrinsic*, *extrinsic*, and *interference*—are modified by the recoil of the final-state hole in the conduction band. We are also interested in studying the effect of plasmon dispersion on the line shape of the satellite band. For the sake of comparison, we have considered photoemission in several different situations. First, we will present our study of the intensity and line shape of the plasmon satellite with and without the hole recoil due to the production of a dispersionless plasmon. Next, we will consider the modifications due to the excitation of a plasmon with dispersion and attenuation.

## II. FORMALISM

We use the recently developed  $T$ -matrix formulation<sup>10,11</sup> to study this problem, as the usual linear theory is unsuitable for a proper description of photoemission. Our model for the metal sample is that of a semi-infinite jellium extending from  $z = -\infty$  to 0. The photoelectron created at depth  $z$  exits from the metal normal to the surface ( $z=0$ ). During this process a plasmon can be excited either *intrinsicly* by the hole created in the conduction band or *extrinsicly* by the photoelectron on its way out of the metal. A negative term occurs due to quantum interference between the *extrinsic* and the *intrinsic* processes. In our formalism, the intensity spectrum of the valence band photoemission accompanied by  $n$  plasmons can be written as<sup>10,11</sup>

$$I_n(\epsilon_k) = \int_{-\infty}^0 dz \rho(z) J_n(\epsilon_k, z), \quad (1)$$

where  $J_n(\epsilon_k, z)$  is the probability that the photoelectron produced at the depth  $z$  leaves the metal surface with an energy  $\epsilon_k$  after  $n$  plasmon productions, and  $\rho(z)$  is the primary ionization density which will be taken to be a constant (equal to 1). In terms of the transit time  $\tau = -z/V_k$  ( $V_k$  being the speed of the photoelectron inside the metal), we can write Eq. (1) as

$$I_n(\epsilon_k) = \int_0^\infty d\tau V_k J_n(\epsilon_k, \tau). \quad (2)$$

The production rate  $J_n(\epsilon_k, \tau)$  can be expressed in terms of the  $T$ -matrix element by using methods discussed in Refs. 10 and 11. All processes contributing to the  $T$ -matrix element are shown in Fig. 1. In this diagram, the incident photon of frequency  $\omega$  is represented by the wavy line. The process of photoemission is shown in terms of the production of a particle-hole pair in the conduction band at time  $t$ . The single line pointing upward represents the propagation of the photoelectron through the metal before its emission from the metal surface at time  $t + \tau$  with energy  $\epsilon_k = k^2/2m$ . The single line pointing downward is the propagator for the hole created in the conduction band. The *extrinsic* plasmon productions are described by the dashed lines attached to the photoelectron propagator while the *intrinsic* plasmon lines are attached to the hole propagator. The *extrinsic* plasmons can be created only between times  $t$ , the instant at which the photoelectron is created, and  $t + \tau$ , the instant at which the photoelectron leaves the surface of the metal (represented by the black dot in Fig. 1). From this diagram, it is obvious that the *extrinsic* terms will not be affected by the recoil of the final-state hole, as they are related to the outgoing photoelectron line. However, we expect that the *intrinsic* and the *interference* terms will be modified by the hole mobility.

In this paper, we will be concerned with single-plasmon production only. In our model, the production rate of photoelectrons along with zero and one plasmon excitations can be written as

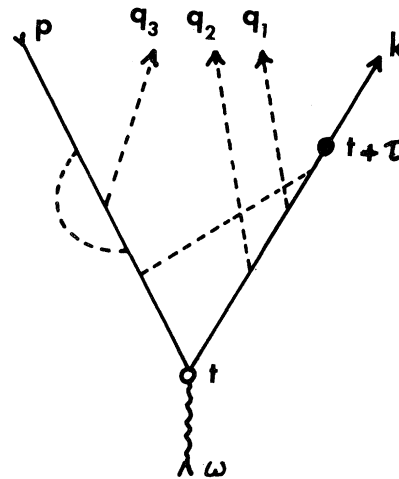


FIG. 1. Diagram representing the process of valence-band photoemission in a metal with *extrinsic* ( $q_1$  and  $q_2$ ) and *intrinsic* ( $q_3$ ) plasmon productions.

$$J_n(\epsilon_k, \tau) = \frac{(4\pi k_F^3/3)^{-1}}{Nn!} \int d\vec{p} \Theta(k_F - p) \times \begin{cases} \delta(\epsilon_k - \epsilon_p - \omega) & \text{for } n=0, \\ \tilde{T}(\epsilon_k, \epsilon_p, \tau) & \text{for } n=1, \end{cases} \quad (3)$$

where  $\Theta$  is the step function and  $k_F$  is the Fermi momentum. The  $T$ -matrix element has the form

$$\tilde{T}(\epsilon_k, \epsilon_p, \tau) = \frac{1}{(2\pi)^3} \int d\vec{q} [g(q)]^2 \delta(\epsilon_k + \omega_p(q) - \epsilon_p - \omega) \times \left| \frac{\Theta(k_F - |\vec{p} - \vec{q}|)}{\mu(\vec{k}, \vec{q})} - \frac{1 - \exp[i\nu(\vec{k}, \vec{q})\tau]}{\nu(\vec{k}, \vec{q})} \right|^2. \quad (4)$$

Here  $\mu^{-1}$  and  $\nu^{-1}$  are, respectively, the propagators related to the internal hole and electron lines appearing in the first-order diagram (see Fig. 1). Factor

$$g(q) = [\frac{1}{2}v(q)\omega_p(q)c(q)]^{1/2}$$

is the plasmon-electron coupling function, where  $v(q) = 4\pi e^2/q^2$  is the Coulomb potential,  $\omega_p(q)$  the plasmon frequency with dispersion,<sup>18</sup> and  $c(q)$  an attenuation function. This attenuation function describes the weakening of the plasmon-electron coupling due to pair excitations as  $q$  approaches the cutoff wave number  $q_c$ , above which the plasmon mode disappears; one has  $c(0) = 1$  and  $c(q_c) = 0$  with  $c(q)$  slightly smaller than one for most of the plasmon momentum range  $0 < |\vec{q}| \lesssim q_c$ .

The normalization factor  $N$  appearing in Eq. (3) is determined by requiring conservation of the number of photoelectrons, i.e., by using

$$\int_{\epsilon_F}^{\omega + \epsilon_F} d\epsilon_k \sum_{n=0}^{\infty} J_n(\epsilon_k, \tau) = 1. \quad (5)$$

$$I_1(\epsilon_k) = D(\epsilon_k) \int d\vec{p} \Theta(k_F - p) \frac{1}{(2\pi)^3} \int d\vec{q} [g(q)]^2 \delta(\epsilon_k + \omega_p(q) - \epsilon_p - \omega) \times \left[ \frac{\Theta(k_F - |\vec{p} - \vec{q}|)}{[\mu(\vec{k}, \vec{q})]^2} - \frac{2\mathcal{P}\Theta(k_F - |\vec{p} - \vec{q}|)}{\mu(\vec{k}, \vec{q})\nu(\vec{k}, \vec{q})} + \frac{2\pi}{\Gamma(\epsilon_k)} \delta(\nu(\vec{k}, \vec{q})) \right], \quad (7)$$

where  $\Gamma(\epsilon_k)$  is the usual decay rate due to plasmon production and can be calculated from

$$\Gamma(\epsilon_k) = \frac{me^2}{k} \int_0^{q_c} dq \Theta \left[ q - \frac{m\omega_p(q)}{k} \right] \frac{\omega_p(q)}{q}. \quad (8)$$

The coefficient  $D(\epsilon_k)$  appearing in Eqs. (6) and (7) is a slowly varying function of  $\epsilon_k$  and can be taken to be constant over the range of  $\epsilon_k$  in which we are interested; we therefore set it equal to 1.

The first term in the square modulus of Eq. (4) represents production of an intrinsic plasmon while the second term denotes plasmon production by an extrinsic process. The cross product of these two terms, of course, corresponds to the interference term as described above. Comparing Eq. (4) with the corresponding equation [Eq. (10) of Ref. 10] for the core-state photoemission case, we observe that while the extrinsic term remains unchanged as expected, the intrinsic and the interference terms are altered by the mobility of the final state hole in the conduction band.

Equation (4) can be easily evaluated for high energy photoelectron emission where we can assume  $\tau \gg \omega_p^{-1}$ . In such a case, the intensities of the main line and the first plasmon satellite are given by

$$I_0(\epsilon_k) = D(\epsilon_k) \int d\vec{p} \Theta(k_F - p) \delta(\epsilon_k - \epsilon_p - \omega) \quad (6)$$

and

### III. CALCULATIONS AND RESULTS

Equations (6) and (7) have been evaluated for sodium with  $\omega_p^0 = 5.91$  eV and  $\epsilon_F = 3.23$  eV for an incoming photon energy  $\omega = 90\omega_p^0 = 532$  eV. The intensity of the main line  $I_0(\epsilon_k)$  calculated by ignoring all interaction effects is given by Eq. (6), which reduces to

$$I_0(\epsilon_k) = 4\pi mp, \quad (9)$$

with

$$0 \leq p = (k^2 - 2m\omega)^{1/2} \leq k_F .$$

For the purpose of comparison with the first plasmon satellite band, we have plotted  $I_0(\epsilon_k)$  in Fig. 2. As expected, the main line intensity is parabolic and has the width of the Fermi energy. Numerical computations for the first plasmon satellite have been performed for several different cases.

(A) *No-recoil—no-plasmon dispersion.* First we assume that the final-state hole does not recoil, i.e., we replace  $|\vec{p} - \vec{q}|$  in Eq. (7) with  $p$ . We also assume that the plasmon is dispersionless and without attenuation such that in Eq. (7)  $\omega_p(q)$  and  $c(q)$  can be replaced by  $\omega_p^0$  and 1, respectively. In this case, the total intensity in the first plasmon satellite takes a simple form

$$I_1(\epsilon_k) = 4\pi m p \left[ \frac{e^2 q_c}{\pi \omega_p^0} - \frac{\pi m e^2}{2k} + 1 \right] \quad (10)$$

with

$$0 \leq p = [2m(\omega_p^0 - \omega) + k^2]^{1/2} \leq k_F .$$

(B) *Recoil—no-plasmon dispersion.* Here we retain the recoil of the final-state hole but still ignore

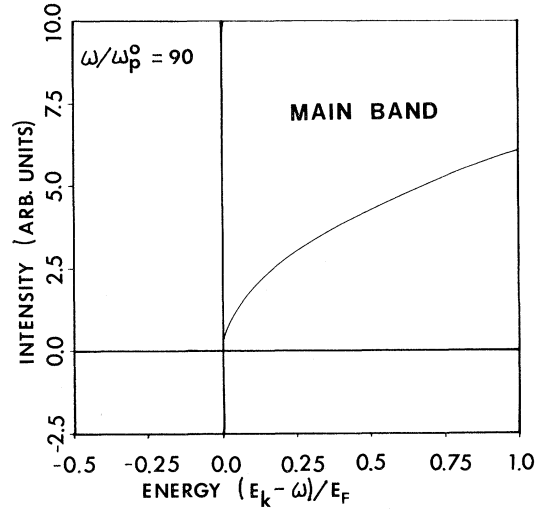


FIG. 2. Line shape of the main band of the valence-band photoemission spectrum of metals, neglecting all interaction effects.

the plasmon dispersion and attenuation. In this case, the intrinsic term is substantially modified and can be expressed as

$$I_1^{\text{intr}}(\epsilon_k) = 4m^3 e^2 \omega_p^0 \int_0^{q_c} \frac{dq}{q} \left[ \frac{1}{2m\omega_p^0 + (q-p)^2 - p^2} - \frac{\Theta(q - k_F + p)}{2m\omega_p^0 - p^2 + k_F^2} - \frac{\Theta(k_F - p - q)}{2m\omega_p^0 + (q+p)^2 - p^2} \right] \quad (11)$$

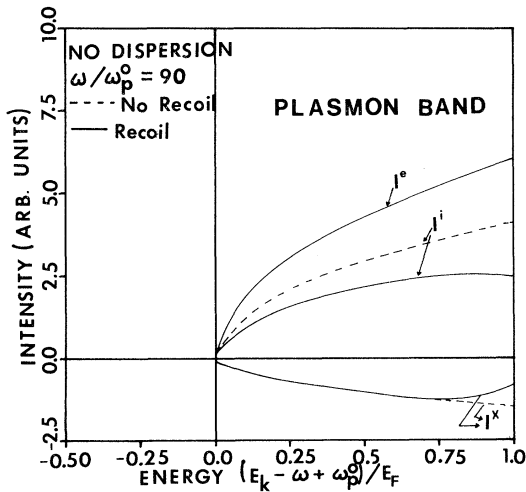


FIG. 3. Intrinsic, extrinsic, and interference contributions to the intensity of the first plasmon satellite for the production of a dispersionless plasmon. The solid and the dashed curves correspond to the cases with recoil and without recoil, respectively.

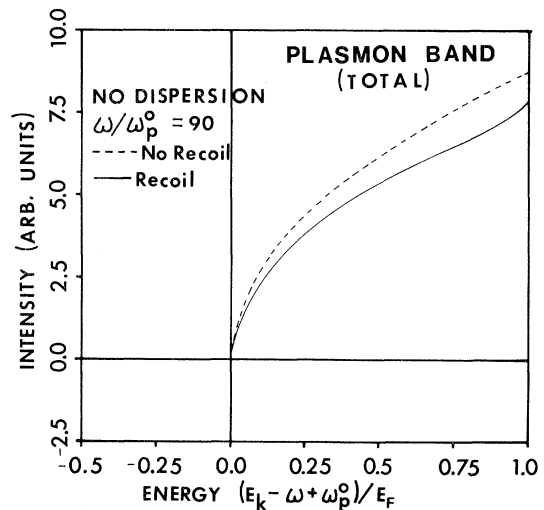


FIG. 4. Line shape of the total intensity of the first plasmon satellite of the valence-band photoemission spectrum for dispersionless plasmon production.

with

$$0 \leq p = [2m(\omega_p^0 - \omega) + k^2]^{1/2} \leq k_F.$$

A similar composite expression for the interference term can also be obtained. The results of the numerical computations for cases (A) and (B) are shown in Figs. 3 and 4. Figure 3 shows the individual contributions of the intrinsic, extrinsic, and interference terms. The solid and dashed lines correspond to the results for the recoil and no recoil cases, respectively. Notice that due to recoil the intrinsic term is substantially reduced. An evaluation of the integrated intensities indicates that this reduction is 29% as previously reported.<sup>13</sup> The interference term has a modest modification near the high-energy edge. As expected, the extrinsic term

remains unaffected by the recoil of the final-state hole. Figure 4 shows the total intensities for these two cases. In this dispersionless plasmon case, the width of the satellite band is the same as that of the main band and the satellite intensity basically reflects the main band intensity. The recoil reduces the overall (integrated) plasmon band intensity by 12.4%. This value is also in accordance with that reported in Ref. 13, in view of the approximations made there.

(C) *No-recoil—exact-plasmon dispersion.* In this case, we again ignore the recoil of the final-state hole ( $|\vec{p} - \vec{q}| \rightarrow p$ ); however, we retain full plasmon dispersion and attenuation.<sup>18</sup> In such a case the total intensity of the plasmon satellite can be calculated from

$$I_1(\epsilon_k) = 4me^2 \int_0^{q_c} dq p c(q) \left[ \frac{1}{\omega_p(q)} - \frac{m}{kq} \ln \left| \frac{m\omega_p(q) + kq - q^2/2}{m\omega_p(q) - kq - q^2/2} \right| + \Theta \left[ q - \frac{m\omega_p(q)}{k} \right] \frac{\pi m\omega_p(q)}{\Gamma(\epsilon_k)kq} \right] \quad (12)$$

with

$$0 \leq p = \{2m[\omega_p(q) - \omega] + k^2\}^{1/2} \leq k_F.$$

(D) *Recoil—exact-plasmon dispersion.* This is the most general case that we consider. We retain both the recoil of the final-state hole and the plasmon dispersion and attenuation. As in case (B), we expect that the intrinsic and the interference terms will be modified by the recoil but the extrinsic term will remain unchanged. In this case the intrinsic term of Eq. (7) can be reduced to

$$I_1^{\text{intr}}(\epsilon_k) = 4m^3 e^2 \int_0^{q_c} dq \frac{\omega_p(q)c(q)}{q} \left[ \frac{1}{2m\omega_p(q) + (q-p)^2 - p^2} - \frac{\Theta(q+p-k_F)}{2m\omega_p(q) + k_F^2 - p^2} - \frac{\Theta(k_F-p-q)}{2m\omega_p(q) + (q+p)^2 - p^2} \right],$$

with

$$0 \leq p = \{2m[\omega_p(q) - \omega] + k^2\}^{1/2} \leq k_F.$$

The interference term of Eq. (7) can be similarly reduced. Numerical computations for cases (C) and (D) have been carried out, again for metallic Na and incident photon energy  $\omega = 90\omega_p^0$ . Results for these cases are shown in Figs. 5 and 6. Figure 5 shows the individual contributions of the intrinsic, extrinsic, and interference terms. The intrinsic term is again significantly reduced by the recoil of the final-state hole. The reduction in the integrated intensity of the intrinsic term is found to be 25.9%. The interference term again undergoes modest modification in the high energy region of the satellite band and there is no change in the extrinsic contribution. Figure 6 shows the total

plasmon band intensities for these two cases. An evaluation of the integrated intensities indicates that recoil reduces the overall intensity by 10.1%. Comparing the results of Figs. 4 and 6, we notice that the plasmon dispersion and attenuation introduce significant modifications in the shape and strength of the satellite band. In the dispersionless case, the shape of the satellite band basically reflects that of the main band and its width is equal to that of the main band. The plasmon dispersion increases the width of the satellite band but weakens its strength. Furthermore, we notice that in the latter case, the intensity goes to zero smoothly at both upper and lower edges. The low-energy tailing of the plasmon band occurs due to the widening of the plasmon frequency by dispersion. The smooth shape of the satellite band near the

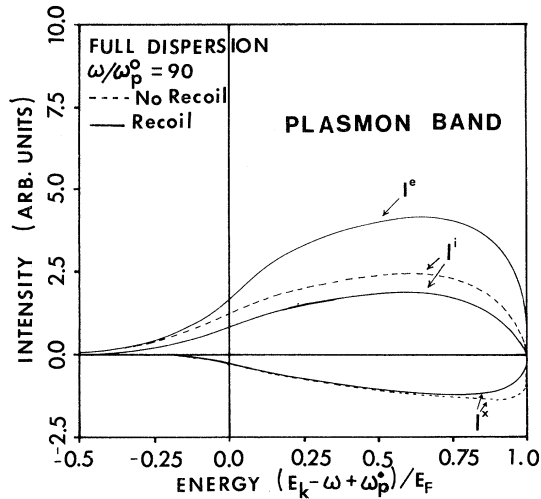


FIG. 5. Intrinsic, extrinsic, and interference terms contributing to the first plasmon satellite intensity for the production of a plasmon with dispersion and attenuation.

upper edge is due to the fact that for all  $q$ ,  $\omega_p(q) \geq \omega_p^0$ , so that the interval of  $q$  between 0 and  $q_c$  which is still consistent with conservation of energy becomes smaller for larger  $\epsilon_k$ . This smoothly brings the spectrum to the point at which no photoemission is allowed.

#### IV. SUMMARY AND CONCLUSIONS

By using the  $T$ -matrix formalism developed recently for the study of the core-level x-ray photoemission spectra of metals, we have investigated the valence-band photoemission spectra of simple metals. The additional feature that we had to introduce to study this problem was the effect of recoil of the final-state hole created in the conduction band. It is found that at high incident photon energies the hole mobility lowers the intensity of the intrinsic term in a significant way and introduces minor modifications in the interference term while the extrinsic contribution remains unaffected. Numerical computations for the main band and the first plasmon satellite have been performed for Na for both the dispersionless plasmon and the plasmon with dispersion and attenuation. In both cases, recoil lowers the total intensity of the satellite band by a significant amount. In the dispersionless plasmon case, the satellite band reflects the main band in its shape and width. In the presence of plasmon dispersion and attenuation, the satellite band becomes weaker in strength but covers a

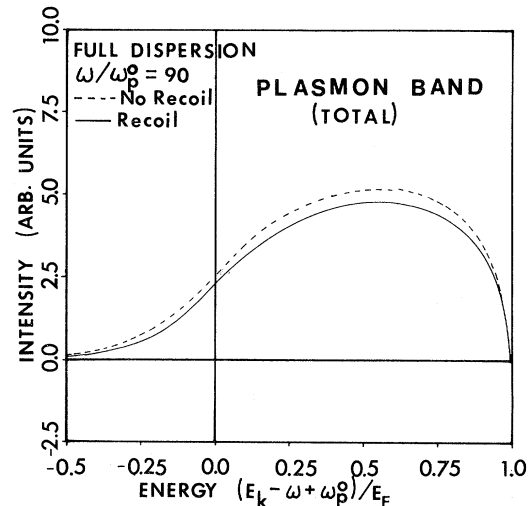


FIG. 6. Total intensity of the first plasmon satellite for the production of a plasmon with dispersion and attenuation.

wider range of energies. In this case, the satellite band intensity goes to zero smoothly at both the upper and lower edges. This can be understood strictly on the basis of energy conservation as discussed in the preceding section.

We are aware of only a few experiments on the valence-band photoemission spectra of simple metals.<sup>16,17</sup> It appears that our theoretical prediction regarding the overall reduction of the strength of the plasmon satellite due to hole recoil has already been verified by an independent experiment of Van Attekum and Trooster.<sup>16</sup> They measured the valence-band photoemission of Al along with the  $s$ - and  $p$ -state photoemissions. By employing a deconvolution technique they obtained the lossless spectra for these cases. From their study they concluded that the strength of the plasmon line for the valence-band photoemission was lower than the core state spectra of the same metal. This qualitatively agrees with our theoretical conclusion.<sup>13</sup> For a detailed comparison with experiments regarding the line shape and width of the plasmon satellite, there must be further carefully conducted experimental studies.

#### ACKNOWLEDGMENT

This work was supported in part by the NATO Research Grant No. 1433 and in part by The Fonds National de la Recherche Scientifique, Belgium.

- <sup>1</sup>R. S. Williams, P. S. Wehner, G. Apai, J. Stöhr, D. A. Shirley, and S. P. Kowalczyk, *J. Electron Spectrosc. Relat. Phenom.* **12**, 477 (1977).
- <sup>2</sup>D. Norman and D. P. Woodruff, *Surf. Sci.* **79**, 76 (1979).
- <sup>3</sup>S. A. Flodstrom, R. Z. Bachrach, R. S. Bauer, J. C. McMenamin, and S. B. M. Hagström, *J. Vac. Sci. Technol.* **14**, 303 (1977).
- <sup>4</sup>L. I. Johansson and I. Lindau, *Solid State Commun.* **29**, 1379 (1979).
- <sup>5</sup>J. C. Fuggle, D. J. Fabian, and L. M. Watson, *J. Electron Spectrosc. Relat. Phenom.* **9**, 99 (1976).
- <sup>6</sup>B. I. Lundqvist, *Phys. Kondens. Mater.* **9**, 236 (1969).
- <sup>7</sup>S. Doniach, and M. Sunjić, *J. Phys. C* **3**, 285 (1970).
- <sup>8</sup>J. Chang and D. C. Langreth, *Phys. Rev. B* **5**, 3512 (1972); D. C. Langreth, in *Collective Properties of Physical Systems*, 24th Nobel Symposium, edited by B. I. Lundqvist and S. Lundqvist (Academic, New York, 1974), p. 210.
- <sup>9</sup>D. R. Penn, *Phys. Rev. Lett.* **38**, 1429 (1977); **40**, 568 (1978).
- <sup>10</sup>D. Chastenet and P. Longe, *Phys. Rev. Lett.* **44**, 91 (1980); **44**, 903 (E) (1980); D. Chastenet, Ph.D. thesis, University of Paris, 1980 (unpublished).
- <sup>11</sup>S. M. Bose, P. Kiehm, and P. Longe, *Phys. Rev. B* **23**, 712 (1981).
- <sup>12</sup>L. Hedin, *Phys. Scr.* **21**, 477 (1980).
- <sup>13</sup>P. Longe and S. M. Bose, *Solid State Commun.* **38**, 527 (1981).
- <sup>14</sup>S. Doniach, *Phys. Rev. B* **2**, 3898 (1970).
- <sup>15</sup>T. McMullen, B. Bergersen, and P. Jena, *J. Phys. C* **9**, 975 (1976).
- <sup>16</sup>P. M. Th. M. Van Attekum and J. M. Trooster, *Phys. Rev. B* **18**, 3872 (1978).
- <sup>17</sup>H. Höchst, P. Steiner, and S. Hüfner, *J. Phys. F* **7**, L309 (1977).
- <sup>18</sup>A. J. Glick and R. A. Ferrell, *Ann. Phys. (N.Y.)* **11**, 359 (1960).